British Journal of Pharmacology (2008) 154, 872–881
 0007–1188/08 $30.00
www.brjpharmacol.org

RESEARCH PAPER

Translocation of the insulin-regulated aminopeptidase to the cell surface: detection by radioligand binding

H Demaegdt[1], L Smitz[1], J-P De Backer[1], MT Le[1], M Bauwens[2], E Szemenyei[3], G Tóth[3], Y Michotte[4], P Vanderheyden[1] and G Vauquelin[1]

[1]*Department of Molecular and Biochemical Pharmacology, Vrije Universiteit Brussel, Brussels, Belgium;* [2]*Department of Medical Imaging and Physical Sciences, Vrije Universiteit Brussel, Brussels, Belgium;* [3]*Institute of Biochemistry, Biological Research Centre, Hungarian Academy of Sciences, University of Szeged, Szeged, Hungary and* [4]*Department of Pharmaceutical Chemistry, Drug Analysis and Drug Information, Vrije Universiteit Brussel, Brussels, Belgium*

Background and purpose: Insulin-regulated aminopeptidase (IRAP) and the insulin-dependent glucose transporter GLUT4 colocalize in specific intracellular vesicles (that is, GLUT4 vesicles). These vesicles move slowly to the cell surface, but their translocation is markedly enhanced by insulin, resulting in higher glucose uptake. Previous studies of the insulin-mediated translocation of IRAP to the cell surface have been hampered by the laborious detection of IRAP at the cell surface. We aimed to develop a more direct and faster method to detect IRAP. To this end, we used model systems with well-characterized IRAP: CHO-K1 cells expressing endogenous IRAP and recombinant HEK293 cells expressing human IRAP. A more widespread application of the method was demonstrated by the use of 3T3-L1 adipocytes.
Experimental approach: After stimulation of the cells with insulin, internalization of IRAP was inhibited by the addition of phenyl arsine oxide (PAO). Then, cell-surface IRAP was detected by the high-affinity binding of radiolabelled angiotensin (Ang) IV (either ^{125}I or ^{3}H).
Key Results: We monitored the time- and concentration dependence of insulin-mediated translocation of IRAP in both cell lines and 3T3-L1 adipocytes. A plateau was reached between 6 and 8 min, and 10^{-7} M insulin led to the highest amount of IRAP at the cell surface.
Conclusions and implications: Based on the capacity of the IRAP apoenzyme to display high affinity for radiolabelled Ang IV and on the ability of PAO to inhibit IRAP internalization, we developed a more direct and faster method to measure insulin-mediated translocation of IRAP to the cell surface.
British Journal of Pharmacology (2008) **154,** 872–881; doi:10.1038/bjp.2008.117; published online 21 April 2008

Keywords: angiotensin IV; IRAP; translocation; radioligand binding; insulin; adipocytes

Abbreviations: Ang, angiotensin; CHO-K1 cells, Chinese hamster ovary cells; HEK293 cells, human embryo kidney cells; IRAP, insulin-regulated aminopeptidase; PAO, phenyl arsine oxide; PI3 kinase, phosphatidyl inositol 3 kinase

Introduction

Insulin-regulated aminopeptidase (IRAP, also denoted as cystinyl aminopeptidase (EC 3.4.11.3)) is a membrane-associated zinc-dependent metallopeptidase of the M1 family. It is well known that IRAP colocalizes with the GLUT4 insulin-dependent glucose transporter in specific intracellular vesicles (that is, GLUT4 vesicles) in adipose tissue and skeletal muscle. These vesicles move slowly to the cell surface, but this translocation is markedly enhanced by insulin, resulting in a higher glucose uptake (Kandror and Pilch, 1994; Mastick *et al*., 1994; Keller *et al*., 1995; Ross *et al*., 1996). This constitutes the major mechanism by which insulin regulates glucose homeostasis.

Insulin-regulated aminopeptidase is thought to have an important role in the sorting and trafficking of GLUT4 storage vesicles. Indeed, injection of the amino terminus of IRAP in 3T3-L1 adipocytes causes GLUT4 translocation to the plasma membrane, possibly through competition with retention or sorting proteins (Waters *et al*., 1997). In agreement with these data, recent studies showed that IRAP knockdown in 3T3-L1

Correspondence: Dr H Demaegdt, Department of Molecular and Biochemical Pharmacology, Vrije Universiteit Brussel, Pleinlaan 2, Brussels, Elsene, Brabant 1050, Belgium.
E-mail: hdemaegd@vub.ac.be
Received 16 January 2008; revised 20 February 2008; accepted 27 February 2008; published online 21 April 2008

adipocytes leads to impairment of GLUT4 translocation and glucose uptake (Yeh *et al.*, 2007). The cytoplasmic tail of IRAP contains numerous targeting motifs (Johnson *et al.*, 2001), and multiple components of the GLUT4 storage vesicle-trafficking machinery were found to interact with IRAP (Katagiri *et al.*, 2002; Tojo *et al.*, 2003; Hosaka *et al.*, 2005; Larance *et al.*, 2005; Peck *et al.*, 2006; Yeh *et al.*, 2007).

There are at least two insulin-dependent signalling pathways that lead to the exocytosis of GLUT4 vesicles in skeletal muscle cells and adipocytes: firstly, a phosphatidyl inositol 3 kinase (PI3 kinase)-dependent pathway that leads to the activation of Akt/protein kinase B and/or atypical protein kinase Cs; and secondly, a PI3 kinase-independent pathway that leads to the activation of the c-Cbl-Cbl-associated protein complex (c-Cbl-CAP), which plays an important role in the membrane fusion of the GLUT4 vesicles (Bryant *et al.*, 2002).

Previous studies of the translocation of IRAP to the cell surface have been hampered by the laborious detection of the enzyme at the cell surface. Direct IRAP identification relied on the precipitation of biotinylated membrane proteins or fractionation, followed by sodium dodecyl sulphate-polyacrylamide gel electrophoresis, western blotting and immunodetection of IRAP (Garza and Birnbaum, 2000; Nakamura *et al.*, 2000). Alternatively, indirect approaches relied on the binding of radiolabelled transferrin to a chimeric protein consisting of the intracellular domain of IRAP and the extracellular domain of the transferrin receptor (Johnson *et al.*, 1998). Using this latter approach, it could be shown that IRAP undergoes insulin-mediated translocation in the CHO cell model system despite the fact that it does not contain measurable amounts of GLUT4 (Johnson *et al.*, 1998; Lampson *et al.*, 2000; Bogan *et al.*, 2001; Lim *et al.*, 2001). Recently, we observed that Chinese hamster ovary (CHO-K1) cells contain a large concentration of endogenous IRAP. In membrane preparations of these cells, we were able to detect IRAP by the high-affinity binding of [^{125}I]-Ang (angiotensin) IV and by measuring its catalytic activity with the substrate L-leucine-*p*-nitroanilide. Enzymatic activity in these membranes was almost completely inhibited by Ang IV (Demaegdt *et al.*, 2004b). In a subsequent study, it was found that human embryo kidney (HEK293) cells have a low endogenic IRAP content and that, when transiently expressed in these cells, human IRAP (hIRAP) shows the same enzymatic and binding characteristics as native IRAP in CHO-K1 cells (Demaegdt *et al.*, 2006).

In this study, we describe a more direct and convenient method to study the translocation of IRAP to the surface of CHO-K1 cells and hIRAP-expressing recombinant HEK293 cells in response to insulin. This method is based on the specific detection of IRAP by radiolabelled Ang IV binding (Demaegdt *et al.*, 2006). To demonstrate a more general application of this method, we also examined the translocation of IRAP in 3T3-L1 adipocytes.

Methods

Cell culture, transient transfection and differentiation

CHO-K1 cells were kindly provided by the Pasteur Institute (Brussels, Belgium) and HEK293 cells from AstraZeneca (Mölndal, Sweden). 3T3-L1 preadipocytes were purchased from ATCC (Teddington, UK).

All cells were cultured in 24-well plates (Greiner, Wemmel, Belgium) in Dulbecco's modified essential medium supplemented with L-glutamine (2 mM), 2% (v/v) of a stock solution containing 5000 IU mL^{-1} penicillin and 5000 μg mL^{-1} streptomycin, 1% (v/v) of a stock solution containing non-essential amino acids, 1 mM sodium pyruvate and 10% (v/v) fetal bovine serum. The cells were grown in 5% CO_2 at 37 °C until confluent.

HEK293 cells were transiently transfected with plasmid DNA, pCIneo, containing the gene of human IRAP. Transient transfections were performed as described previously with 8 μl mL^{-1} Lipofectamine and 1 μg mL^{-1} plasmid DNA (Le *et al.*, 2005). After transfection, the cells were cultured for 2 more days. IRAP-transfected HEK293 cells displayed eight times higher enzyme activity than non-transfected cells.

Twenty-four hours before the experiment, the medium from CHO-K1 and transfected HEK293 cells was replaced by serum-free medium.

3T3-L1 preadipocytes were differentiated before the experiments were started (Zhang *et al.*, 2004). Two days after confluency (day 0), cells were stimulated with MDI (methylxanthine, dexamethasone, insulin) induction media (0.5 mM isobutylxanthine, 1 μg mL^{-1} insulin, 1 μM dexamethasone). Two days later (day 2), the medium was changed to one with supplemented Dulbecco's modified essential medium plus 1 μg mL^{-1} insulin. At day 4, the medium was changed to supplemented Dulbecco's modified essential medium and cells were fed every 2 days with this medium. Cells were used for experiments at days 8 and 9. Three hours before the experiment, 3T3-L1 adipocytes were deprived of serum.

Cell viability was tested by using Trypan blue. Cells were washed with phosphate-buffered saline (PBS) and then trypsinized. Trypan blue (dissolved in PBS) was added to a final concentration of 0.1% and the dead (blue) and living cells were counted with the use of a microscope and a Bürker haemacytometer.

Translocation assay and detection of IRAP

After the cells had been washed twice with PBS, they were incubated at 37 °C in medium (50 mM Tris-HCl (pH 7.4) containing 140 mM NaCl, 300 μl per well) in the absence (control) or presence of insulin. These incubations were performed with different concentrations of insulin (10^{-9}–10^{-5} M) for a fixed time (6 min) or with one concentration of insulin (10^{-7} M) for different incubation times (0–20 min). Subsequently, cells were placed on ice and washed once with cold PBS.

To avoid internalization of IRAP at the surface, 400 μl medium containing 10 or 50 μM phenyl arsine oxide (PAO) was added, and the cells were preincubated on ice for 10 min. Then, 50 μl of a mixture of EDTA and 1,10-phenantrolin (both 100 μM final concentration), 50 μl of medium without or with unlabelled Ang IV (to determine the nonspecific binding) and 50 μl of [^{125}I]-Ang IV and [^{3}H]-Ang IV (final concentration of 1 and 5 nM, respectively) were added. Radioligand binding was performed at 37 °C for 30 and 40 min, respectively.

After the cells had been washed three times with cold PBS to remove the free radioligand, they were dissolved in 300 μl of NaOH (1 M) for 1 h at room temperature. Finally, after addition of 200 μl of water, the supernatant was transferred and radioactivity was measured in a γ- or β-counter depending on the radioligand used ([^{125}I]-Ang IV or [^{3}H]-Ang IV, respectively).

In preliminary experiments, internalized and cell-surface binding could be differentiated by mild acid treatment, as mentioned in a previous study (Fierens *et al*., 1999; Vanderheyden *et al*., 1999). Cells were treated twice, for 5 min on ice, with 500 μl of glycine buffer (30 mM glycine, 125 mM NaCl, pH 3). The supernatants were combined, representing the cell-surface binding. The internalized fraction corresponded to the remaining radioactivity in the cells. This fraction was dissolved in 300 μl of NaOH (1 M) for 1 h at room temperature, and finally 200 μl of water was added. In all subsequent experiments, IRAP internalization was completely inhibited by PAO, so the mild acid treatment could be omitted (that is, cells were immediately dissolved in NaOH after the incubation with the radioligand).

Binding studies on cell membranes

Crude membrane homogenates of CHO-K1 and hIRAP-expressing HEK293 cells (hIRAP-HEK293) were used to study the potential effect of PAO on radioligand binding. The membranes were prepared as previously described (Demaegdt *et al*., 2004b). For binding, the membrane pellets were thawed and resuspended using a Polytron homogenizer in 50 mM Tris-HCl (pH 7.4) binding buffer containing 140 mM NaCl. The incubations were carried out in polyethylene 24-well plates (Elscolab, Kruibeke, Belgium) in a final volume of 300 μl per well consisting of 150 μl membrane homogenate (corresponding to 4×10^5 CHO-K1 cells per well and 1.5×10^5 hIRAP-HEK293 cells per well), 50 μl of an EDTA/1,10-phenanthrolin mixture, both with a final concentration of 100 μM, 50 μl binding buffer (for total binding), PAO (final concentrations from 0 to 100 μM) or 10 μM unlabelled Ang IV (for nonspecific binding). Subsequently, 50 μl [^{125}I]-Ang IV or [^{3}H]-Ang IV was added at a final concentration of 1 and 5 nM, respectively. After 60 min incubation at 37 °C, the mixture was vacuum filtered using a Inotech 24-well cell harvester through glass fibre filters (Whatman) presoaked in 1% (w/v) BSA. After drying, the radioactivity retained in the filters was measured using a Perkin-Elmer γ-counter, in the case of [^{125}I]-Ang IV, or a β-counter for [^{3}H]-Ang IV (after addition of 3 mL scintillation liquid).

Data analysis and statistical procedures

All experiments were performed at least three times with triplicate determinations in each. When mentioned, a one-way ANOVA was performed to determine the significance with Graphpad Prism 4 (Figures 5 and 7c). A statistically significant difference was detected at <0.01, and therefore, Dunnett's *post hoc* test was performed to compare each condition with the control.

Drugs and other materials

Angiotensin IV (that is, Ang II (3–8)) was obtained from NeoMPS (Strasbourg, France), and Tyr^4 of Ang IV was iodinated using the Iodogen iodination reagent from Pierce (Erembodegem, Belgium), as described by Lahoutte *et al*. (2003). ^{125}I was obtained from MP Biomedicals (Asse, Belgium). Monoiodinated Ang IV was isolated on a Grace Vydac C_{18} monomeric 120A reverse-phase HPLC column and stored at −20 °C in 10 mM KH_2PO_4, pH 6.5, containing 45% ethanol.

$^{3,4}\Delta$Pro^5-Ang IV precursor peptide was synthesized by the solid-phase peptide synthesis method using Fmoc chemistry. Tritiation was carried out in a self-designed vacuum manifold by the catalytic saturation of $^{3,4}\Delta$Pro^5-Ang IV, using a method described previously (Tóth *et al*., 1997). $^{3}H_2$ gas was purchased from Technobexport (Moscow, Russia), and it contained ⩾98% tritium. The total activity of the crude [^{3}H]-Pro^5- IV was 2.79 GBq (75.5 mCi). The radioactivity of the tritiated peptide was measured with a TRI-CARB 2100TR liquid scintillation counter in a toluene–Triton X-100 cocktail. [^{3}H]-Pro^5-Ang IV was purified by HPLC using a Grace Vydac 218TP54 C_{18} column on a Jasco Radio-HPLC instrument, and liquid scintillation detection was performed on a Canberra Packard Radiomatic 505TR Flow Radiochromatography Detector with the Ultima-Flo M scintillation cocktail. The specific activity of the pure labelled peptide was determined by HPLC using a standard peptide calibration curve to 1.5 TBq mmol^{-1} (40.8 Ci mmol^{-1}).

Streptomycin, fetal bovine serum and Lipofectamine were purchased from Invitrogen (Merelbeke, Belgium). pCIneo containing the gene of human cystinyl aminopeptidase was kindly provided by Professor M Tsujimoto (Laboratory of Cellular Biochemistry, Saitama, Japan). The scintillation liquid used was Optiphase Hisafe from Perkin-Elmer (Boston, MA, USA). All other reagents were of the highest grade commercially available.

Results

Distinction between cell-surface and internalized radiolabelled Ang IV binding and effect of PAO thereon

Previously, internalized and cell-surface binding of [^{3}H]-Ang II to AT_1 (Angiotensin Type 1) receptor-expressing recombinant CHO-K1 cells could be differentiated by treating the cells with mild acid (glycine buffer, pH 3) on ice (Fierens *et al*., 1999; Vanderheyden *et al*., 1999). In these experiments, only the cell-associated radioligand molecules that were accessible to the acid (that is, those present at the cell surface) came into solution. Based on the observation that the radiolabelled Ang IV (both tritiated and iodinated) that was bound to membranes in CHO-K1 cell homogenates was also fully released in the presence of glycine buffer (data not shown), this mild acid treatment was adopted to differentiate internalized from cell-surface-bound radiolabelled Ang IV in the initial experiments with intact cells.

In these and all ensuing experiments, intact CHO-K1 cells were incubated for 30 min at 37 °C with [^{125}I]-Ang IV and intact, recombinant HEK293 cells that transiently express

hIRAP (hIRAP-HEK293 cells) were incubated for 40 min at 37 °C with [^{3}H]-Ang IV (Table 1). As shown in Figure 1, a large proportion of bound radioligand was resistant to mild acid treatment and hence can be considered to be internalized. When the cells were pretreated on ice for 10 min with PAO before the addition of the radioligand (Table 1, steps 1–4), the internalization of the radioligand could be completely prevented. The decrease in acid-resistant binding was dependent on the PAO concentration and coincided with an increased acid-sensitive binding. Interestingly, CHO-K1 cells were more sensitive to this treatment than the hIRAP-HEK293 cells. Although 10 μM PAO fully prevented radioligand internalization in the CHO-K1 cells, it only partially prevented internalization in the hIRAP-HEK293 cells, where 50 μM PAO was needed. In the ensuing experiments, the cells were pretreated with these low PAO concentrations to prevent radioligand internalization. As internalization was completely blocked by PAO, mild acid treatment was no longer required to quantify the cell-surface binding of radiolabelled Ang IV (Table 1, steps 1–3).

In control experiments performed to assess the potential cytotoxic effects of PAO (Gibson *et al*., 1989), both cell types were incubated with different concentrations of PAO, trypsinized and treated with Trypan blue. As shown in Figure 2, more than 80% of the cells survive even in the presence of 50 μM PAO. The potential influence of PAO on the binding of radiolabelled Ang IV was studied by making use of membrane homogenates of CHO-K1 and hIRAP-HEK293 cells. PAO induced a limited increase in [^{125}I]-Ang IV binding to CHO-K1 cell membranes but had no effect on [^{3}H]-Ang IV binding to hIRAP-HEK293 cell membranes (Figure 3).

Table 1 Procedure for measuring the translocation of IRAP

		CHO-K1 cells		*hIRAP-HEK293 cells*	
	Condition	*Treatment*	*Time (min)*	*Treatment*	*Time (min)*
1	37 °C	Insulin	0–20	Insulin	0–20
2[a]	Ice	10 μM PAO	10	50 μM PAO	10
3	37 °C	1 nM [^{125}I]Ang IV	30	5 nM [^{3}H]Ang IV	40
4[b]	Ice	Glycine	2 × 5	Glycine	2 × 5

Abbreviations: CHO-K1, Chinese hamster ovary cells; HEK293, human embryo kidney cells; IRAP, insulin-regulated aminopeptidase; PAO, phenyl arsine oxide.
[a]In Figure 1, the concentration of PAO varied between 0 and 100 μM.
[b]This step was only executed in Figure 1.

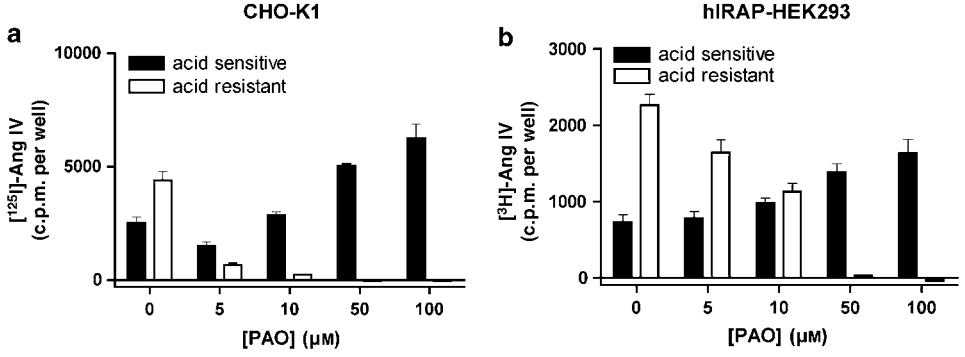

Figure 1 Effect of PAO on cell-surface and internalized binding of radiolabelled Ang IV. Intact CHO-K1 (**a**) and recombinant HEK293 (**b**) cells were treated as mentioned in Table 1 (steps 1–4). Data refer to specific binding calculated by subtracting nonspecific binding in the presence of 10 μM unlabelled Ang IV from total binding. Values are the average ± s.e.mean of a representative experiment of two experiments with triplicate determinations in each. Ang, angiotensin; CHO-K1, Chinese hamster ovary cells; HEK293, human embryo kidney cells; PAO, phenyl arsine oxide.

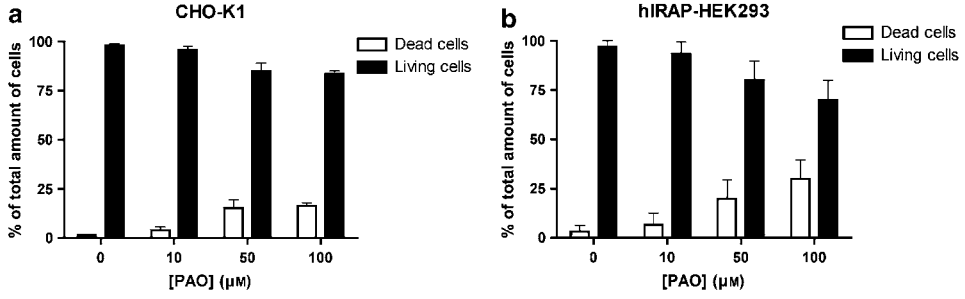

Figure 2 Cytotoxic effect of PAO. CHO-K1 (**a**) and hIRAP-HEK293 (**b**) cells were treated with different concentrations of PAO for 10 min on ice and 40 min at 37 °C. After being washed, the cells were trypsinized and treated with Trypan blue. Values are expressed as a percentage of the total amount of cells (dead/stained and alive). Data are the average ± s.d. of two experiments with triplicate determinations in each. Ang, angiotensin; CHO-K1, Chinese hamster ovary cells; HEK293, human embryo kidney cells; IRAP, insulin-regulated aminopeptidase; PAO, phenyl arsine oxide.

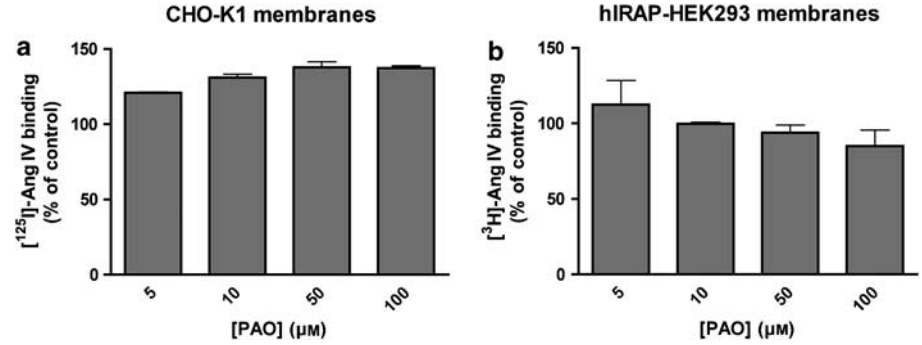

Figure 3 Effect of PAO on the high-affinity binding of Ang IV. CHO-K1 (**a**) and recombinant HEK293 (**b**) membrane homogenates were incubated with different concentrations of PAO and binding was performed for 1 h at 37 °C in the presence of 1 nM [^{125}I]-Ang IV or 5 nM [^{3}H]-Ang IV, respectively. Binding is expressed as a percentage of specific control binding (control, no PAO). Values are the average ± s.d. of two experiments with triplicate determinations in each. Ang, angiotensin; CHO-K1, Chinese hamster ovary cells; HEK293, human embryo kidney cells; PAO, phenyl arsine oxide.

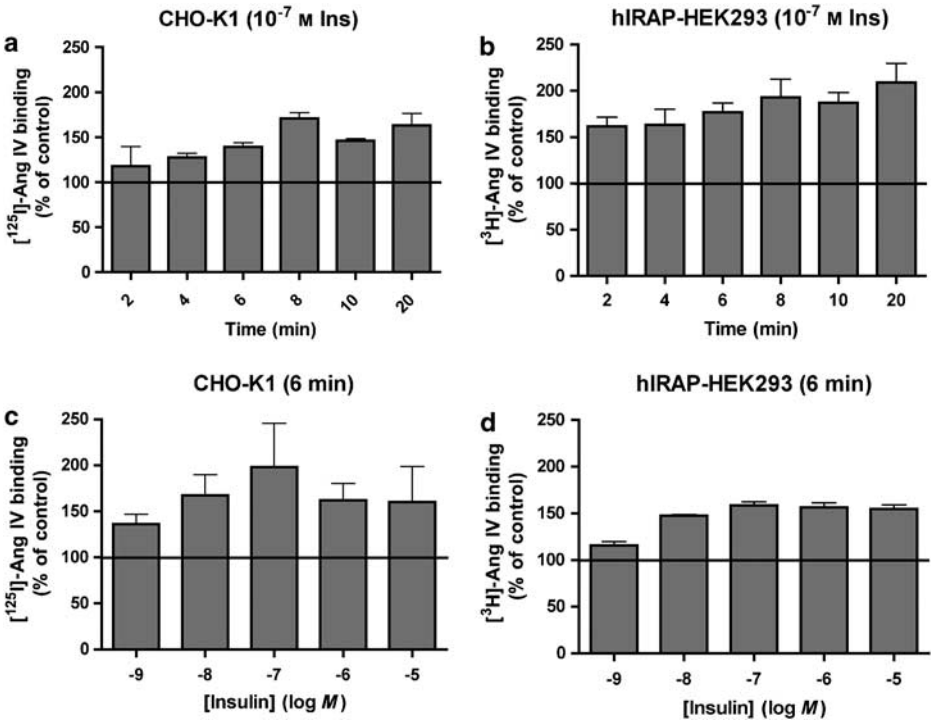

Figure 4 Translocation of IRAP to the cell surface after treatment of the cells with insulin. (**a** and **b**) Effect of incubation time on the response to 10^{-7} M insulin. CHO-K1 (**a**) and recombinant HEK293 (**b**) cells were incubated with insulin for different time periods. (**c** and **d**) Effect of the insulin concentration on the binding of [^{3}H]Ang IV. CHO-K1 (**c**) and recombinant HEK293 (**d**) cells were incubated with different concentrations of insulin for 6 min. Subsequently, all cells were further treated as mentioned in Table 1 (steps 1–3). Data refer to specific binding, expressed as a percentage of the control (no insulin). Values are the average ± s.e.mean of three experiments with determinations performed in triplicate. Ang, angiotensin; CHO-K1, Chinese hamster ovary cells; HEK293, human embryo kidney cells; IRAP, insulin-regulated aminopeptidase.

Insulin-mediated translocation of IRAP to the cell surface in CHO-K1 and hIRAP-HEK293 cells

Using the new approach described above (Table 1, steps 1–3), we measured the translocation of IRAP (that is, radiolabelled Ang IV binding sites) to the cell surface in response to insulin. To explore the time dependence of the insulin effect, CHO-K1 and hIRAP-HEK293 cells were pretreated (that is, before PAO treatment and radioligand binding) at 37 °C with a fixed concentration of insulin (0.1 μM) for increasing periods of time up to 20 min. As depicted in Figure 4a, insulin produced a time-dependent increase in [^{125}I]-Ang IV binding to the surface of CHO-K1 cells until a plateau level was reached after about 6–8 min of incubation. A similar pattern was observed when examining [^{3}H]-Ang IV binding to hIRAP-HEK293 cells (Figure 4b), except that the binding was already markedly increased after a 2 min exposure to insulin.

To investigate the concentration dependence of the insulin effect, cells were pretreated at 37 °C for a fixed time (6 min) with increasing concentrations of insulin up to

10 μM. Binding of labelled Ang IV to both CHO-K1 cells (Figure 4c) and hIRAP-HEK293 cells (Figure 4d) was already significantly increased by 1 nM insulin and the increase was maximal when the cells were exposed to insulin concentrations ranging between 10 nM and 10 μM.

As a control, experiments were also performed with inversed radioligand/cell type combinations. After a 6-min incubation with 0.1 μM insulin, a comparable increase of cell-surface binding was observed for both radioligands in each cell line, that is, 136.3 ± 3.9 and 139.1 ± 4.8% in CHO-K1 cells and 177.0 ± 9.7 and 158.4 ± 14.6% in hIRAP-HEK293 cells for [^{3}H]-Ang IV and [^{125}I]-Ang IV, respectively ($n = 3$).

Taken together, these experiments illustrate the ability of insulin to produce a time- and concentration-dependent increase in the cell-surface localization of IRAP in both cell types.

Sensitivity of the insulin-stimulated IRAP translocation to wortmannin and LY294.002

To verify that insulin stimulates the translocation of IRAP through the classic PI3 kinase pathway, we examined the effect of the PI3 kinase inhibitors wortmannin and LY294.002 thereon (Arcaro and Wymann, 1993). To this end, the stimulation of CHO-K1 and hIRAP-HEK293 by insulin (0.1 μM, 6 min, 37 °C) was preceded by a 15-min treatment with 0.1 μM wortmannin or 50 μM LY294.002 at 37 °C. The experiment was further performed as depicted in Table 1 (steps 1–3). As shown in Figure 5, pretreatment with these PI3 kinase inhibitors completely prevented the insulin-induced translocation of IRAP in both cell lines. After this pretreatment, the cell-surface IRAP concentration was the same in the presence or absence of insulin. This concentration was the same as under control conditions (that is, native cells) for hIRAP-HEK293 cells but lower for CHO-K1 cells.

Translocation in 3T3-L1 adipocytes

As a test for a more widespread applicability of the present detection method, we examined the insulin-mediated translocation of IRAP to the cell surface of 3T3-L1 adipocytes using 5 nM [^{3}H]-Ang IV as tracer and 50 μM PAO to prevent internalization (internalization was completely prevented under this condition; Figure 6). A comparison of the data presented in Figures 4, 7a and b reveals that the insulin-mediated translocation is much more pronounced in the 3T3-L1 adipocytes than in the CHO-K1 and hIRAP-HEK293 cells. In all three cell lines, maximal translocation was seen after 6–8 min and with 10^{-7} M insulin. Pretreatment of the 3T3-L1 adipocytes with only LY294.002 did not affect [^{3}H]-Ang IV binding, but wortmannin produced a modest increase. Yet both PI3 kinase inhibitors almost completely blocked the effect of insulin (Figure 7c).

Discussion and conclusion

In this study, we describe for the first time a direct method to detect IRAP at the cell surface. This method facilitates the study of factors affecting the translocation of IRAP from intracellular stores to the cell surface in response to insulin

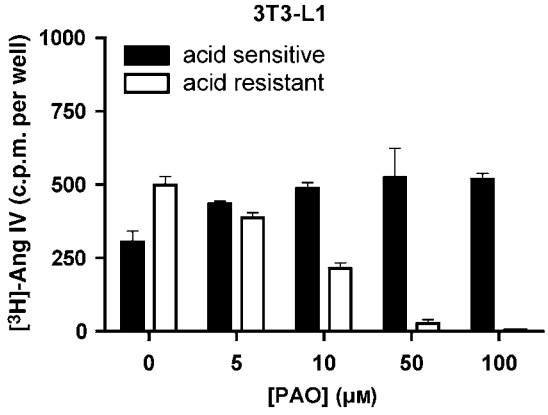

Figure 6 Effect of PAO on the cell-surface and internalized binding of radiolabelled Ang IV to 3T3-L1 adipocytes. The experiments were performed as in Figure 1. Ang, angiotensin; PAO, phenyl arsine oxide.

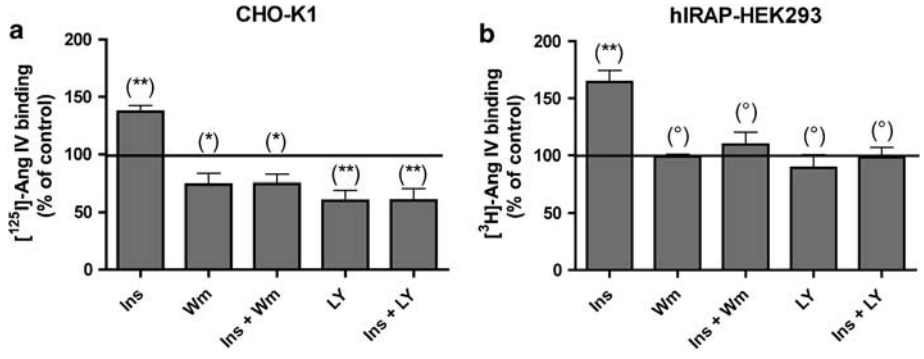

Figure 5 Effect of wortmannin and LY294.002 on insulin-stimulated translocation of IRAP to the cell surface. CHO-K1 (**a**) and recombinant HEK293 (**b**) cells were preincubated for 15 min with 0.1 μM wortmannin (Wm) or 50 μM LY294.002 (Ly) and then stimulated with 10^{-7} M insulin (Ins) for 6 min at 37 °C. Cells were further treated as outlined in Table 1 (steps 1–3). Data refer to specific binding after normalization according to the control (without wortmannin, LY294.002 or insulin treatment). Values are the average ± s.e.mean of three experiments with triplicate determinations in each. The differences between control and different conditions were determined by using one-way ANOVA and Dunnett's *post hoc* test: **$P<0.01$; *$P<0.05$; °$P>0.05$, not significantly different. CHO-K1, Chinese hamster ovary cells; HEK293, human embryo kidney cells; IRAP, insulin-regulated aminopeptidase.

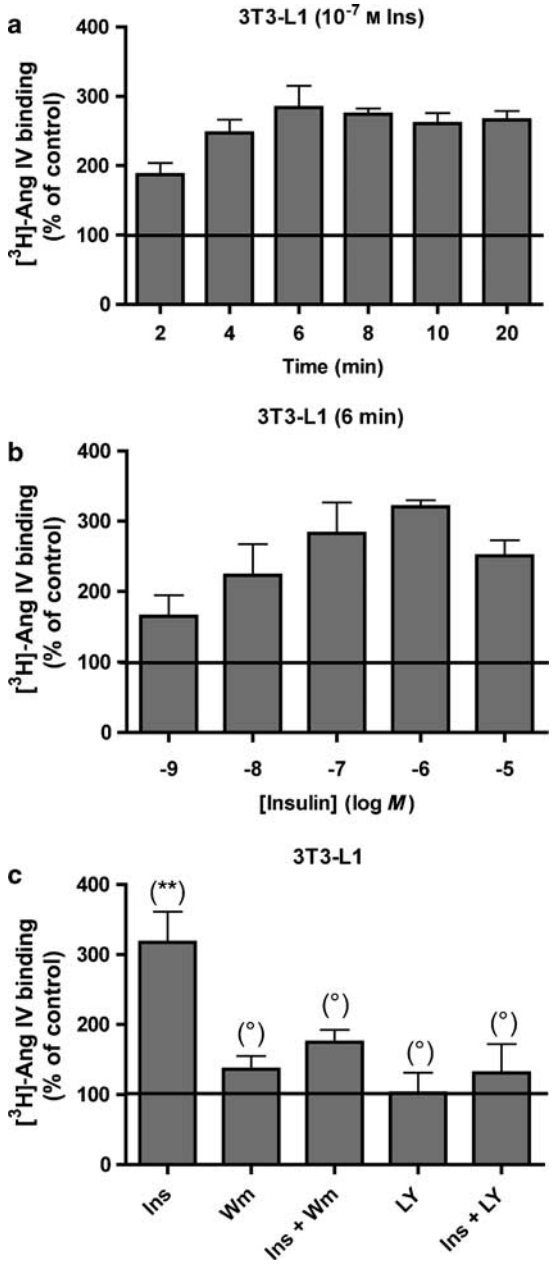

Figure 7 Translocation of IRAP to the cell surface after treatment of 3T3-L1 adipocytes with insulin. 3T3-L1 adipocytes were incubated with (**a**) 10^{-7} M insulin for different time periods or (**b**) different concentrations of insulin for 6 min. Subsequently, all cells were further treated as shown in Table 1 (steps 1–3). (**c**) 3T3-L1 adipocytes were pretreated with wortmannin or LY294.002 and then stimulated with 10^{-7} M insulin for 6 min. The experiments were performed as in Figure 5. Data refer to specific binding, expressed as a percentage of the control (no insulin). Values are the average ± s.e.mean of three experiments with determinations performed in triplicate. The differences between control and different conditions were determined by using one-way ANOVA and Dunnett's *post hoc* test: $^{**}P<0.01$; $^{*}P<0.05$; $^{\circ}P>0.05$, not significantly different. IRAP, insulin-regulated aminopeptidase.

and other stimuli. It is based on the specific binding of radiolabelled Ang IV to the IRAP apoenzyme (Demaegdt *et al*., 2004a, 2006; Laeremans *et al*., 2005). As tools, we compared the binding of [^{125}I]-Ang IV and [^{3}H]-Ang IV. Assays were developed using CHO-K1 cells with endogenous IRAP and hIRAP-HEK293 cells expressing recombinant hIRAP and then applied for the detection of IRAP at the surface of 3T3-L1 adipocytes.

Previously, the detection of IRAP at the cell surface relied on time-consuming multistep procedures, involving the precipitation of biotinylated membrane proteins or fractionation, followed by sodium dodecyl sulphate-polyacrylamide gel electrophoresis, western blotting and immunodetection with anti-IRAP antibodies (Garza and Birnbaum, 2000; Nakamura *et al*., 2000). IRAP translocation was also studied in CHO-K1 cells, but its detection relied on an indirect approach based on the binding of radiolabelled transferrin to a chimeric protein consisting of the intracellular domain of IRAP and the extracellular domain of the transferrin receptor (Johnson *et al*., 1998). These studies revealed that despite the lack of detectable GLUT4 transporters in these cells, they possess the machinery that is responsible for the insulin-mediated translocation of IRAP to the cell surface (Johnson *et al*., 1998; Lampson *et al*., 2000; Bogan *et al*., 2001; Lim *et al*., 2001). In the light of these findings, we were pleasantly surprised to find that CHO-K1 cells contain endogenous IRAP and that the concentration of this enzyme is even fairly high compared to the other cell lines we studied (Demaegdt *et al*., 2004b, 2006). Only hIRAP-HEK293 contained higher amounts of recombinant IRAP (Demaegdt *et al*., 2006).

A link between IRAP and the hexapeptide Ang IV was first described by Albiston *et al*. (2001). In a search for the putative 'Ang IV receptors', these authors demonstrated that IRAP constitutes the major binding site of a photoactive radiolabelled analogue of Ang IV. Subsequent binding studies with [^{125}I]-Ang IV on crude cell membranes of hIRAP-HEK293 cells revealed that IRAP displays the same pharmocological properties as the Ang IV receptors in a variety of other non-transfected cell lines and tissue extracts (Handa *et al*., 1999; Lew *et al*., 2003; Demaegdt *et al*., 2006). Of note, these binding studies were all performed in the presence of the divalent cation chelators EDTA and 1,10-phenanthrolin. The necessity for these (or chemically related) chelators for obtaining high-affinity [^{125}I]-Ang IV binding to IRAP has recently been explained by the finding that such binding only takes place to the catalytic zinc-depleted IRAP apoenzyme (Demaegdt *et al*., 2004a; Laeremans *et al*., 2005). Based on the identical pharmacological profile of the labelled sites in different studies, as well as the absence of specific binding in HEK293 cells expressing recombinant aminopeptidase N, the IRAP apoenzyme appears to be the sole candidate for high-affinity [^{125}I]-Ang IV binding, and this selectivity greatly facilitates the specific detection of this enzyme (Demaegdt *et al*., 2006).

Here, we show that this binding technique allows the selective detection of IRAP at the cell surface when the cells have been pretreated with PAO (Figures 1 and 6), a reagent well known for its ability to block the endocytosis of cell-surface proteins by disrupting the structure of clathrin-coated pits (Hertel *et al*., 1985; Griendling *et al*., 1987; Grady *et al*., 1995; Rückert *et al*., 2003; Visser *et al*., 2004). In this respect, our findings confirm the conclusion of Garza and Birnbaum (2000) that IRAP internalization in adipocytes is most likely clathrin mediated. The PAO concentrations used

in this study have only a minimal effect on cell integrity and radioligand binding (Figures 2 and 3).

In the absence of PAO pretreatment, internalized and cell-surface [^{125}I]-Ang IV–IRAP complexes in the cells investigated can still be discriminated from each other, because only the latter are susceptible to rapid dissociation in a mild acidic environment (Figures 1 and 6). This mode of discrimination has been sought on several occasions to monitor the internalization of [^{3}H]-Ang II–AT$_1$ receptor complexes, and it has also been used once in a study on Ang IV receptor internalization (Briand *et al*., 1999). Although this approach is not universally applicable (Fierens *et al*., 2001), we show here that it is valid in the case of the Ang IV–IRAP combination.

New in this study is the IRAP apoenzyme that can also be detected by the high-affinity binding of [^{3}H]-Ang IV. Compared to the traditional use of [^{125}I]-Ang IV in such studies, the disadvantage of the low specific radioactivity of [^{3}H]-Ang IV is certainly counterbalanced by its very low degree of nonspecific binding (that is, less than 20% as compared to up to 50% for [^{125}I]-Ang IV in intact cell binding; data not shown). Although only the [^{125}I]-Ang IV–CHO-K1 and [^{3}H]-Ang IV–hIRAP-HEK293 cell combinations were extensively studied here for the detection of IRAP and its translocation, similar observations were obtained with the two other radioligand–cell combinations. Although the nature of the radioligand seems to matter with respect to the degree of nonspecific binding and the amount of counts, it does not seem to influence the extent of insulin-mediated translocation.

Most importantly, both labelled forms of Ang IV can be used to study the effect of stimuli such as insulin on the translocation of IRAP to the cell surface, as well as the effect of compounds affecting the intracellular processes involved. By consecutively treating the cells with insulin, PAO (on ice) and radioligand (Table 1, steps 1–3), insulin was shown to produce a similar time- and concentration-dependent increase of the IRAP concentration at the surface of CHO-K1 and hIRAP-HEK293 cells and 3T3-L1 adipocytes. At 37 °C, a plateau was reached after about 6–8 min, and 10^{-7} M insulin led to the highest amount of IRAP at the cell surface (Figures 4 and 7). Similar optimal conditions have also been observed for the translocation of recombinant GLUT4 in CHO-K1 cells (Kanai *et al*., 1993; Bogan *et al*., 2001) and endogenous GLUT4 in 3T3-L1 adipocytes (Bogan *et al*., 2001). Insulin could only raise the surface concentration of IRAP to 1.5 times the initial amount in CHO-K1 and hIRAP-HEK293 cells, whereas at least three times the initial amount was seen for the 3T3-L1 adipocytes. The presently observed translocation of IRAP in insulin-stimulated 3T3-L1 adipocytes is not yet as high as that seen in some other studies based on alternative IRAP detection techniques (5–8 times increase in the studies by Ross *et al*., 1996; Garza and Birnbaum, 2000; Zeigerer *et al*., 2002), but it correlates well with preliminary experiments by us revealing a four-time increase in glucose uptake (data not shown). The quantitative differences in IRAP translocation seen in the present and earlier studies could be explained by exploring the influence of the degree/conditions of 3T3-L1 adipocyte differentiation, culture conditions or even the origin of the cells.

The effect of different concentrations of insulin after 6 min (Figures 4c, d and 7b) was analysed according to a single-site model (that is, a sigmoidal dose–response curve). This yielded ED_{50} values in the nanomolar range (0.9 ± 0.1, 2.2 ± 0.1 and 2.8 ± 0.2 nM for CHO-K1 cells, hIRAP-HEK293 cells and 3T3-L1 adipocytes, respectively). This range is in agreement with that found in the literature for recombinant GLUT4 translocation in CHO cells (Kanai *et al*., 1993).

In adipocytes, skeletal muscle cells, as well as other cell types, it has been shown that insulin increases the cell-surface GLUT4 and IRAP concentrations by stimulating the translocation of GLUT4 vesicles and that the PI3 kinase-related pathway is the main factor in this process (Herman *et al*., 1994; Lampson *et al*., 2000; Bryant *et al*., 2002). In agreement, this pathway seems to be responsible for most of the insulin-mediated increase in cell-surface IRAP concentration in the three cell lines investigated. Indeed, the stimulating effect of insulin could be completely blocked by the PI3 kinase inhibitors wortmannin (Arcaro and Wymann, 1993) and LY294.002 (Liang *et al*., 2000) in CHO-K1 and hIRAP-HEK293 cells and to a large extent in 3T3-L1 adipocytes (Figures 5 and 7c). Although not significant ($P > 0.05$) from a statistical point of view, wortmannin did not completely inhibit the effect of insulin in the 3T3-L1 adipocytes. However, it is unlikely that this implies that an alternative pathway is responsible for this effect. Indeed, a PI3 kinase-independent pathway leading to protein TC10 activation and membrane fusion of the GLUT4 vesicles has been found to be required for glucose uptake in these cells, but it does not appear to be sufficient to induce the effect of insulin (Chiang *et al*., 2001; Bryant *et al*., 2002).

Alternative techniques could be used for the detection of cell-surface IRAP. The first one is based on the ability of this enzyme to cleave a number of synthetic substrates such as L-leucine-*p*-nitroanilide and on the ability of Ang IV to block this process. Yet compared to binding studies with radiolabelled Ang IV, this approach was found to suffer from its limited ability to discriminate between IRAP and related metalloproteases such as aminopeptidase N (Demaegdt *et al*., 2006). Similar considerations can be advanced for the cell-impermeable substrate lysyl-AMC-glutathione (Ross *et al*., 1996). Finally, cell-surface IRAP could also be detected by using commercial antibodies directed against its extracellular C-terminal region. Yet we and others (C SY (University of Melbourne, Melbourne, VIC, Australia) and M Ruiz-Ortega (Universidad Autónoma Madrid, Madrid, Spain), personal communication) have had only limited success in using these antibodies with a variety of cell systems.

In conclusion, the present experiments illustrate the ability of insulin to produce a time- and concentration-dependent increase in the exposure of IRAP at the surface of CHO-K1 cells, recombinant HEK293 cells expressing hIRAP and 3T3-L1 adipocytes. These experiments rely on a newly developed method, based on radiolabelled Ang IV binding, to detect cell-surface IRAP. This simple approach could be used for monitoring the translocation of IRAP in the presence of insulin or other stimuli such as insulin-like growth factor-1 in these and other cell systems as well as the effect of certain (patho)physiological conditions thereon.

Acknowledgements

We are most obliged to the Research Council of the 'Vrije Universiteit Brussel' (GOA-2002), the 'Fonds voor Wetenschappelijk Onderzoek Vlaanderen' and the 'Geneeskundige Stichting Koningin Elisabeth' for their financial support. HD has received a grant from the 'Institute for the Promotion of Innovation through Science and Technology in Flanders' (IWT-Vlaanderen) and PV is the recipient of a VUB research fellowship. We are also very grateful to Ken Kersemans (Department of Medical Imaging and Physical Sciences, Vrije Universiteit Brussel) for ^{125}I labelling of Ang IV. GT thanks the financial support of Grant OTKA 046514 from the Hungarian Research Foundation. We also thank Professor D Maes (Vrije Universiteit Brussel) for advice in the statistical analysis.

Conflict of interest

The authors state no conflict of interest.

References

Albiston AL, McDowall SG, Matsacos D, Sim P, Clune E, Mustafa T *et al*. (2001). Evidence that the angiotensin IV (AT(4)) receptor is the enzyme insulin-regulated aminopeptidase. *J Biol Chem* **276**: 48623–48626.

Arcaro A, Wymann MP (1993). Wortmannin is a potent phosphatidylinositol 3-kinase inhibitor: the role of phosphatidylinositol 3,4,5-trisphosphate in neutrophil responses. *Biochem J* **296**: 297–301.

Bogan JS, McKee AE, Lodish HF (2001). Insulin-responsive compartments containing GLUT4 in 3T3-L1 and CHO cells: regulation by amino acid concentrations. *Mol Cell Biol* **21**: 4785–4806.

Briand SI, Neugebauer W, Guillemette G (1999). Agonist-dependent AT(4) receptor internalization in bovine aortic endothelial cells. *J Cell Biochem* **75**: 587–597.

Bryant NJ, Govers R, James DJ (2002). Regulated transport of the glucose transporter GLUT4. *Nat Rev Mol Cell Biol* **3**: 267–277.

Chiang SH, Baumann CA, Kanzaki M, Thurmond DC, Watson RT, Neudauer CL *et al*. (2001). Insulin-stimulated GLUT4 translocation requires the CAP-dependent activation of TC10. *Nature* **410**: 944–948.

Demaegdt H, Laeremans H, De Backer JP, Mosselmans S, Le MT, Kersemans V *et al*. (2004a). Synergistic modulation of cystinyl aminopeptidase by divalent cation chelators. *Biochem Pharmacol* **68**: 893–900.

Demaegdt H, Lenaerts PJ, Swales J, De Backer JP, Laeremans H, Le MT *et al*. (2006). AT4 receptor ligand interaction with cystinyl aminopeptidase and aminopeptidase N: [^{125}I]Ang IV only binds to the cystinyl aminopeptidase apoenzyme. *Eur J Pharmacol* **546**: 19–27.

Demaegdt H, Vanderheyden PML, De Backer JP, Mosselmans S, Laeremans H, Le MT *et al*. (2004b). Endogenous cystinyl aminopeptidase in Chinese hamster ovary cells: characterization by [(125)I]Ang IV binding and catalytic activity. *Biochem Pharmacol* **68**: 885–892.

Fierens FL, Vanderheyden PM, De Backer JP, Vauquelin G (1999). Binding of the antagonist [^{3}H]candesartan to angiotensin II AT1 receptor-transfected Chinese hamster ovary cells. *Eur J Pharmacol* **367**: 413–422.

Fierens FL, Vanderheyden PM, Roggeman C, De Backer JP, Thekkumkara TJ, Vauquelin G (2001). Tight binding of the angiotensin AT(1) receptor antagonist [^{3}H]candesartan is independent of receptor internalization. *Biochem Pharmacol* **61**: 1227–1235.

Garza LA, Birnbaum MJ (2000). Insulin-responsive aminopeptidase trafficking in 3T3-L1 adipocytes. *J Biol Chem* **275**: 2560–2567.

Gibson AE, Noel RJ, Herlihy JT, Ward WF (1989). Phenylarsine oxide inhibition of endocytosis: effects on asialofetuin internalization. *Am J Physiol* **257**: 182–184.

Grady EF, Slice LW, Brant WO, Walsh JH, Payan DG, Bunnett NW (1995). Direct observation of endocytosis of gastrin releasing peptide and its receptor. *J Biol Chem* **270**: 4603–4611.

Griendling KK, Delafontaine P, Rittenhouse SE, Gimbrone Jr MA, Alexander RW (1987). Correlation of receptor sequestration with sustained diacylglycerol accumulation in angiotensin II-stimulated cultured vascular smooth muscle cells. *J Biol Chem* **262**: 14555–14562.

Handa RK, Harding JW, Simasko SM (1999). Characterization and function of the bovine kidney epithelial angiotensin receptor subtype 4 using angiotensin IV and divalinal angiotensin IV as receptor ligands. *J Pharmacol Exp Ther* **291**: 1242–1249.

Herman GA, Bonzelius F, Cieutat AM, Kelly RB (1994). A distinct class of intracellular storage vesicles, identified by expression of the glucose transporter GLUT4. *Proc Natl Acad Sci USA* **91**: 12750–12754.

Hertel C, Coulter SJ, Perkins JP (1985). A comparison of catecholamine-induced internalization of beta-adrenergic receptors and receptor-mediated endocytosis of epidermal growth factor in human astrocytoma cells. Inhibition by phenylarsine oxide. *J Biol Chem* **60**: 12547–12553.

Hosaka T, Brooks CC, Presman E, Kim SK, Zhang Z, Breen M *et al*. (2005). p115 Interacts with the GLUT4 vesicle protein, IRAP, and plays a critical role in insulin-stimulated GLUT4 translocation. *Mol Biol Cell* **16**: 2882–2890.

Johnson AO, Lampson MA, McGraw TE (2001). A di-leucine sequence and a cluster of acidic amino acids are required for dynamic retention in the endosomal recycling compartment of fibroblasts. *Mol Biol Cell* **12**: 367–381.

Johnson AO, Subtil A, Petrush R, Kobylarz K, Keller SR, McGraw TE (1998). Identification of an insulin-responsive, slow endocytic recycling mechanism in Chinese hamster ovary cells. *J Biol Chem* **273**: 17968–17977.

Kanai F, Nishioka Y, Hayashi H, Kamohara S, Todaka M, Ebina Y (1993). Direct demonstration of insulin-induced GLUT4 translocation to the surface of intact cells by insertion of a c-myc epitope into an exofacial GLUT4 domain. *J Biol Chem* **268**: 14523–14526.

Kandror KV, Pilch PF (1994). gp160, a tissue-specific marker for insulin-activated glucose transport. *Proc Natl Acad Sci USA* **91**: 8017–8021.

Katagiri H, Asano T, Yamada T, Aoyama T, Fukushima Y, Kikuchi M *et al*. (2002). Acyl-coenzyme A dehydrogenases are localized on GLUT4-containing vesicles via association with insulin-regulated aminopeptidase in a manner dependent on its dileucine motif. *Mol Endocrinol* **16**: 1049–1059.

Keller SR, Scott HM, Mastick CC, Aebersold R, Lienhard GE (1995). Cloning and characterization of a novel insulin-regulated membrane aminopeptidase from Glut4 vesicles. *J Biol Chem* **270**: 23612–23618.

Laeremans H, Demaegdt H, De Backer JP, Le MT, Kersemans V, Michotte Y *et al*. (2005). Metal modulation of cystinyl aminopeptidase. *Biochem J* **390**: 351–357.

Lahoutte T, Mertens J, Caveliers V, Franken PR, Everaert H, Bossuyt A (2003). Comparative biodistribution of iodinated amino acids in rats: selection of the optimal analog for oncologic imaging outside the brain. *J Nucl Med* **44**: 1489–1494.

Lampson MA, Racz A, Cushman SW, McGraw TE (2000). Demonstration of insulin-responsive trafficking of GLUT4 and vpTR in fibroblasts. *J Cell Sci* **113**: 4065–4076.

Larance M, Ramm G, Stockli J, van Dam EM, Winata S, Wasinger V *et al*. (2005). Characterization of the role of the Rab GTPase-activating protein AS160 in insulin-regulated GLUT4 trafficking. *J Biol Chem* **280**: 37803–37813.

Le MT, De Backer JP, Hunyady L, Vanderheyden PM, Vauquelin G (2005). Ligand binding and functional properties of human angiotensin AT(1) receptors in transiently and stably expressed CHO-K1 cells. *Eur J Pharmacol* **513**: 35–45.

Lew RA, Mustafa T, Ye S, McDowall SG, Chai SY, Albiston AL (2003). Angiotensin AT4 ligands are potent, competitive inhibitors

of insulin regulated aminopeptidase (IRAP). *J Neurochem* **86**: 344–350.

Liang L, Jiang J, Frank SJ (2000). Insulin receptor substrate-1-mediated enhancement of growth hormone-induced mitogen-activated protein kinase activation. *Endocrinology* **141**: 3328–3336.

Lim SN, Bonzelius F, Low SH, Wille H, Weimbs T, Herman GA (2001). Identification of discrete classes of endosome-derived small vesicles as a major cellular pool for recycling membrane proteins. *Mol Biol Cell* **12**: 981–995.

Mastick CC, Aebersold R, Lienhard GE (1994). Characterization of a major protein in GLUT4 vesicles. Concentration in the vesicles and insulin-stimulated translocation to the plasma membrane. *J Biol Chem* **269**: 6089–6092.

Nakamura H, Itakuara A, Okamura M, Ito M, Iwase A, Nakanishi Y *et al*. (2000). Oxytocin stimulates the translocation of oxytocinase of human vascular endothelial cells via activation of oxytocin receptors. *Endocrinology* **141**: 4481–4485.

Peck GR, Ye S, Pham V, Fernando RN, Macaulay SL, Chai SY *et al*. (2006). Interaction of the Akt substrate, AS160, with the glucose transporter 4 vesicle marker protein, insulin-regulated aminopeptidase. *Mol Endocrinol* **20**: 2576–2583.

Ross SA, Scott HM, Morris NJ, Leung WY, Mao F, Lienhard GE *et al*. (1996). Characterization of the insulin-regulated membrane aminopeptidase in 3T3-L1 adipocytes. *J Biol Chem* **271**: 3328–3332.

Rückert P, Bates SR, Fisher AB (2003). Role of clathrin- and actin-dependent endocytotic pathways in lung phospholipid uptake. *Am J Physiol Lung Cell Mol Physiol* **284**: 981–989.

Tojo H, Kaieda I, Hattori H, Katayama N, Yoshimura K, Kakimoto S *et al*. (2003). The Formin family protein, formin homolog over-expressed in spleen, interacts with the insulin-responsive aminopeptidase and profilin IIa. *Mol Endocrinol* **17**: 1216–1229.

Tóth G, Lovas S, Ötvös F (1997). Tritium labelling of neuropeptides. In: Irvine GB, Williams CH (eds). *Methods in Molecular Biology, Neuropeptide Protocols*. Humana Press: New Jersey, pp 219–230.

Vanderheyden PM, Fierens FL, De Backer JP, Fraeyman N, Vauquelin G (1999). Distinction between surmountable and insurmountable selective AT1 receptor antagonists by use of CHO-K1 cells expressing human angiotensin II AT1 receptors. *Br J Pharmacol* **126**: 1057–1065.

Visser CC, Stevanovic S, Voorwinden L, Gaillard PJ, Crommelin DJ, Danhof M *et al*. (2004). Validation of the transferrin receptor for drug targeting to brain capillary endothelial cells *in vitro*. *J Drug Target* **12**: 145–150.

Waters SB, D'Auria M, Martin SS, Nguyen C, Kozma LM, Luskey KL (1997). The amino terminus of insulin-responsive aminopeptidase causes Glut4 translocation in 3T3-L1 adipocytes. *J Biol Chem* **272**: 23323–23327.

Yeh TYJ, Sbodio JI, Tsun ZY, Luo B, Chi NW (2007). Insulin-stimulated exocytosis of GLUT4 is enhanced by IRAP and its partner tankyrase. *Biochem J* **402**: 279–290.

Zeigerer A, Lampson MA, Karylowski O, Sabatini DD, Adesnik M, Ren M *et al*. (2002). GLUT4 retention in adipocytes requires two intracellular insulin-regulated transport steps. *Mol Biol Cell* **13**: 2421–2435.

Zhang JW, Tang OO, Vinson C, Lane MD (2004). Dominant-negative C/EBP disrupts mitotic clonal expansion and differentiation of 3T3-L1 preadipocytes. *Proc Natl Acad Sci USA* **101**: 43–47.